Several-temperature systems: extended irreversible thermodynamics and thermal wavefront propagation

Joaquim Fort†, Toni Pujol†‡ and A S Cukrowski§‖

† Departament de Física, Campus de Montilivi, Universitat de Girona, 17071 Girona, Catalonia, Spain
‡ Departament de Física (Física Estadística), Universitat Autònoma de Barcelona, 08193 Bellaterra, Catalonia, Spain
§ Institute of Physical Chemistry, Polish Academy of Sciences, ul. Kasprzada 44/52, 01-224 Warsaw, Poland
‖ Faculty of Mathematical and Natural Sciences, Pedagogical University, ul. Checinska 5, 25-020 Kielce, Poland

Abstract. We develop an extension of local-equilibrium thermodynamics for systems with components at different temperatures. The description includes heat conduction, diffusion, a chemical reaction and heat losses. The ensuing equations are applied to the problem of thermal wavefront propagation. There is satisfactory agreement between the predicted and the experimental values for the speed of combustion flames over cellulosic fuels. Heat losses cause a decrease of the front speed. This generalizes Zeldovich's result. For radiative losses, the effect can easily be about 15%. When the finite speed of thermal signals is taken into account, an additional lowering of the thermal wavefront speed results.

1. Introduction

The components of mixtures have different temperatures in many physical [1–3] chemical [4], climatological [5] and astrophysical [6] phenomena. Some examples are neutron thermalization processes [1], shock waves [2], laser heating of metals [7], plasmas [3, 6, 8], typical chemical reactions [4, 9, 10], electron swarms in gases [11] and solute–solvent systems [12]. Classical irreversible thermodynamics (CIT) is capable of describing the phenomenology of such systems [13] provided that the local thermodynamic equilibrium (LTE) assumption [14] is a valid approximation.

In order to cope with non-LTE states, CIT has been generalized in a variety of situations, such as heat conduction, viscous flow, diffusion, electrical conduction, chemical reactions and reaction–diffusion systems [15–22]. However, such extended irreversible thermodynamics (EIT) models invariably assume a single temperature for the system under consideration so that many interesting phenomena (such as those mentioned above) still lie out of the formalism of EIT. One of our purposes here is to tackle this problem: in section 2.2 we develop a model, in the lines of EIT, which generalizes the current CIT description of several-temperature systems. In both the CIT and EIT descriptions (sections 2.1 and 2.2, respectively), we will also allow for energy source terms, which for the sake of definiteness we shall consider due to a chemical reaction. Our attention will focus on a special situation, namely that in which the reacting species have a different temperature than that of an additional, nonreacting component. For

the sake of mathematical simplicity, we will introduce some additional simplifications that enable us to see very clearly the differences between the CIT and EIT descriptions, as well as to compare with experiment (section 4).

Several-temperature systems with energy source terms for the different components arise in, e.g., typical chemical reactions [4,9,10,23]. Another example can be found in astrophysical models of accretion flows, where protons have a much higher temperature than electrons; here protons react, producing neutral and charged pions [6]. As a third example, one may consider a partly ionized gas. Electrons and ions react (ionization and recombination), but have a slow rate of energy transfer (because of their very different masses), so that they have different temperatures and heat fluxes in general; in this case electrons release energy to a third component, namely neutral atoms [24]. Also, in plasmas under electric fields, the electrons (and ions) can react with a higher temperature than that of the neutral particles. In hot-atom chemistry, atoms produced in nuclear transformations acquire states of higher temperature than that of their surrounding molecules [25]. Yet another example is combustion waves in fuel mixtures that are either highly diluted in an inert component [26] or contain macroscopic particles (see sections 2 and 4). There are also biophysical applications such as forest fire models, which have been treated as a reaction–diffusion process [27] in spite of being essentially driven by the interplay of reaction and heat conduction (instead of diffusion). Forest fires are a special case of combustion waves. In simple, two-dimensional forest fire models there will again appear a heat loss to an inert component (the soil) in addition to the combustion taking place in the grass or trees (the average temperature of which will be higher than that of the soil). As a last example of several-temperature systems with energy sources and an equilibration process, we mention metals irradiated by laser pulses: heat is mainly transported by electrons, which lose energy to the lattice. In this specific example, the energy source corresponds not to a chemical reaction but to a laser heat source [7,28]†. Therefore, the analysis of several-temperature systems with energy sources and/or temperature equilibration processes among components is not of purely academic interest but can be relevant in many different phenomena. The unification of the thermodynamical properties of such different systems is appealing in its own right, and section 2 is devoted to this purpose. As mentioned above, we have decided to make some assumptions that will be explained below in more detail, since in this way we can find reasonably simple results that can be used in the future to develop more general and complicated models.

As an application of the thermodynamic model of section 2, we shall analyse the propagation of thermal wavefronts (section 3). Whereas the propagation of reaction wavefronts has aroused much interest in diffusive systems [27, 29–34], wavefront propagation in conducting systems is also a relevant problem (e.g. in the propagation of combustion waves). The equations derived from CIT and EIT (section 2) are applied in section 3 to analyse the propagation of thermal wavefronts. This allows us to generalize previously known results by incorporating effects related (i) to heat losses and (ii) to the boundness of the speed of heat conduction. In section 3 we predict a law for the decrease of the propagation velocity due to the heat losses (in both the CIT and EIT descriptions) and an additional decrease due to the finite speed of propagation of thermal signals (which cannot be obtained from CIT but does result from the EIT approach). Finally, in section 4 we outline an application of the EIT model, we apply the CIT approach to predict the speed of thermal fronts in a special case (flame spread over cellulosic fuels), compare with the corresponding experimental results and estimate the effects of radiative losses. Section 5 is devoted to concluding remarks.

---

† See also the third paper in [17].

2. Thermodynamical approach

The general form for the law of balance of energy is [14]

$$\frac{\partial}{\partial t}(\rho u) = -\vec{\nabla} \cdot \vec{J} \tag{1}$$

where t is the time, ρ is the density, u is the total energy per unit mass of the system and $\vec{J}$ is the total energy flux. We will analyse a multicomponent matter system by following steps analogous to those used for radiation–matter systems [35, 36]. Let us consider a mixture of components A, B, C, D, ... In order to develop a simple model, we make some assumptions which we indicate in their proper context.

(i) We will consider the case in which component A is inert. For the sake of definiteness, let us consider the case in which components B, C and D react according to

$$\nu_B B + \nu_C C \rightarrow \nu_D D \tag{2}$$

where ν_B, ν_C and ν_D are the stoichiometric coefficients. We assume that the reacting components share a common temperature,

$$T_B = T_C = T_D \tag{3}$$

whereas the nonreacting component A has temperature T_A. Chemical reactions in the presence of a carrier gas (component A in our notation) with its own temperature have been widely studied [23] (some specific examples of physical phenomena in which they arise have been mentioned in section 1). Different temperatures in a single system are not easy to measure experimentally. Indeed, the assumption of a single temperature T_B for the reacting species will make it possible to compare with experiment (section 4).

(ii) Again for the sake of mathematical simplicity, we assume that the overall mixture is macroscopically at rest (i.e. it has vanishing barycentric velocity, $\vec{v} = 0$), and that $\vec{q}_A \approx 0$, $\vec{q}_C \approx 0$, $\vec{q}_D \approx 0$, . . . , i.e. that heat is transported by component B. This happens, for instance, in the laser heating of metals, where the heat flux is due to electrons, whereas the conduction of heat by phonons is negligible [7]. It also happens in many combustion systems over solid fuels, where heat conduction typically takes place mainly in one of the components (either the fuel or the gas). This depends on the relative values of their thermal parameters at the typical pressures and temperatures of the system [37].

Under the assumptions made, equation (1) can be written as

$$\frac{\partial}{\partial t}(\rho u) = -\vec{\nabla} \cdot \vec{q}_B. \tag{4}$$

Concerning the energy evolution of the components, it can be handled in a similar way to the equation for the complete mixture. We have for component B

$$\frac{\partial}{\partial t}(\rho_B u_B) = -\vec{\nabla} \cdot \vec{q}_B + F_B + \alpha_{AB} \tag{5}$$

where the partial density ρ_B is the mass of component B per unit volume of the system, u_B is the energy of B per unit mass of B and

$$F_B = -\nu_B \nu_{ch} E_B \tag{6}$$

is the energy source term, with ν_{ch} the chemical rate of reaction (2). E_B denotes the mean (kinetic plus electronic) energy of a molecule of species B (see, e.g., [38]). Similarly, we can introduce ρ_i and E_i for the reacting species $i = C, D$. Since the energy must be conserved in reaction (2) we have [38]

$$\nu_B E_B + \nu_C E_C = \nu_D E_D. \tag{7}$$

In equation (5) α_{AB} is the rate of energy transfer from component A to component B per unit volume of the system, and it will depend on their temperatures. It can be calculated from kinetic-theoretical models for dilute [39] and dense [40] gases, for the interaction between electrons and the phonon lattice in metals [7], etc. For the sake of completeness we give the microscopic expression for α_{AB} in a relevant case, namely that corresponding to energy losses from a reactive gas component B to macroscopic or mesoscopic particles A. Then, the energy lost per unit time and volume can be estimated as the number of collisions (per unit time and volume) multiplied by the mean energy exchange per collision, resulting in [41, 42]

$$\alpha_{AB} = \frac{\pi r^2}{\sqrt{\pi}} \frac{c_v P}{R} \sqrt{\frac{8k}{m_B T_B}} a_f n_A (T_A - T_B) \tag{8}$$

where r is the mean radius of the particles A, c_v the molar specific heat of gas B at constant volume, P its pressure, R the universal gas constant, m_B the molecular mass of gas B and a_f the Knudsen accommodation factor ($a_f < 1$), which takes into account the fact that gas molecules do not become thermalized with the particles after a single collision [42]. n_A is the number density of mesoscopic particles A and k is the Boltzmann constant.

Before going ahead, let us stress that the theory presented in sections 2 and 3 does not rely on a specific microscopic expression for α_{AB}.

Concerning components C and D, we have, analogously to equation (5) and making use of (3),

$$\frac{\partial}{\partial t}(\rho_C u_C) = F_C + \alpha_{AC} \tag{9}$$

$$\frac{\partial}{\partial t}(\rho_D u_D) = F_D + \alpha_{AD} \tag{10}$$

where for the reaction (2) we have (analogously to equation (6))

$$F_C = -\nu_C \nu_{ch} E_C \tag{11}$$

$$F_D = \nu_D \nu_{ch} E_D. \tag{12}$$

The equation of balance of energy for species A can be obtained from equations (4), (5), (9) and (10), taking into account that

$$\rho u = \rho_A u_A + \rho_B u_B + \rho_C u_C + \rho_D u_D. \tag{13}$$

This yields

$$\frac{\partial}{\partial t}(\rho_A u_A) = -\alpha_A \tag{14}$$

where we have defined $\alpha_A \equiv \alpha_{AB} + \alpha_{AC} + \alpha_{AD}$, and used equation (7).

In the next two sections, we derive evolution equations according to CIT and generalize them in the framework of EIT.

2.1. CIT

In CIT, the system is assumed to be in LTE [14], i.e. the local specific entropy depends on the same variables as in equilibrium. In order to express this in mathematical terms, we recall that the CIT approach to radiation–matter systems in [35, 36] was constructed by assuming that the entropy per unit mass depends on the matter energy per unit mass and on the radiation energy *also per unit mass of matter*. This theory, which is in agreement with microscopic results [43], can be readily generalized to multicomponent matter systems by assuming the specific entropy of the system to depend on the energies of the components per unit *total*

mass. In addition, the entropy will also depend on the concentrations, which change over time because of the chemical reaction (2). We do not include global density changes because, as mentioned above, we consider the overall system to be at rest macroscopically, thus the specific volume is constant. We can express these ideas in the form of an equation for the time rate of change for the entropy per unit mass,

$$\frac{ds_{le}}{dt} = \sum_i \frac{1}{T_i} \frac{d\hat{u}_i}{dt} - \sum_i \frac{\mu_i}{T_i} \frac{d\hat{c}_i}{dt} \tag{15}$$

where the subscript $_{le}$ to the specific entropy s denotes local equilibrium. We have defined

$$\hat{u}_i \equiv \rho_i u_i / \rho = \hat{c}_i u_i \tag{16}$$

as the energy of component i per unit mass of the *whole* system, and

$$\hat{c}_i \equiv \rho_i / \rho \tag{17}$$

are the concentrations (or mass fractions). The thermodynamical temperatures T_i and chemical potentials μ_i of the components are defined by

$$\frac{1}{T_i} \equiv \frac{\partial s_{le}}{\partial \hat{u}_i} \tag{18}$$

$$\mu_i \equiv -T_i \frac{\partial s_{le}}{\partial \hat{c}_i} \tag{19}$$

respectively. The definitions (18) are analogous to the corresponding ones for radiation–matter systems, introduced in section 3 of [36].

Equation (5) can be expressed in terms of the new partial energy variable $\hat{u}_B$ as follows:

$$\rho \frac{\partial \hat{u}_B}{\partial t} = -\vec{\nabla} \cdot \vec{q}_B + F_B + \alpha_{AB}. \tag{20}$$

The same can be done with equations (9), (10) and (14). Insertion of the equations thus derived into (15), and use of equations (3), (6), (7), (11) and (12), yields

$$\rho \frac{ds_{le}}{dt} = -\frac{\vec{\nabla} \cdot \vec{q}_B}{T_B} + \alpha_A \left(\frac{1}{T_B} - \frac{1}{T_A} \right) - \frac{\mu_A}{T_A} \frac{d\hat{c}_A}{dt} - \frac{1}{T_B} \left(\mu_B \frac{d\hat{c}_B}{dt} + \mu_C \frac{d\hat{c}_C}{dt} + \mu_D \frac{d\hat{c}_D}{dt} \right) \tag{21}$$

where we have recalled the definition $\alpha_A \equiv \alpha_{AB} + \alpha_{AC} + \alpha_{AD}$ as well as equation (3). The last term in equation (21) may be rewritten in terms of the local-equilibrium chemical affinity of the reaction (2), namely

$$A_{le} \equiv \mu_B m_B \nu_B + \mu_C m_C \nu_C - \mu_D m_D \nu_D \tag{22}$$

(m_i is the molecular mass of component i), by making use of the balance equations for the mass fractions [14, 15],

$$\rho \frac{d\hat{c}_B}{dt} = -m_B v_{ch} \nu_B - \vec{\nabla} \cdot \vec{J}_B \tag{23}$$

$$\rho \frac{d\hat{c}_C}{dt} = -m_C v_{ch} \nu_C - \vec{\nabla} \cdot \vec{J}_C \tag{24}$$

$$\rho \frac{d\hat{c}_D}{dt} = m_D v_{ch} \nu_D - \vec{\nabla} \cdot \vec{J}_D \tag{25}$$

$$\rho \frac{d\hat{c}_A}{dt} = 0 \tag{26}$$

where $\vec{J}_i$ is the diffusive flux for species $i = B, C, D$. In equation (26), we have assumed $\vec{J}_A \simeq 0$, i.e. a uniform distribution of the nonreacting species: this can be easily generalized,

but it will make the calculations in section 3 simpler and adequate to compare with experiment (section 4). In the way explained above, we obtain

$$\rho \frac{\mathrm{d}s_{\mathrm{le}}}{\mathrm{d}t} = -\frac{\vec{\nabla} \cdot \vec{q}_{\mathrm{B}}}{T_{\mathrm{B}}} + \alpha_{\mathrm{A}} \left(\frac{1}{T_{\mathrm{B}}} - \frac{1}{T_{\mathrm{A}}} \right) + \sum_i \frac{\mu_i}{T_{\mathrm{B}}} \vec{\nabla} \cdot \vec{J}_i + \frac{v_{\mathrm{ch}} A_{\mathrm{le}}}{T_{\mathrm{B}}}. \tag{27}$$

Comparison with the general law of balance of entropy, namely,

$$\rho \frac{\mathrm{d}s_{\mathrm{le}}}{\mathrm{d}t} = -\vec{\nabla} \cdot \vec{J}_{\mathrm{le}}^s + \sigma_{\mathrm{le}}^s \tag{28}$$

leads to the following identifications for the local-equilibrium entropy flux $s\,\vec{J}_{\mathrm{le}}^s$ and entropy production rate σ_{le}^s:

$$\vec{J}_{\mathrm{le}}^s = \frac{\vec{q}_{\mathrm{B}}}{T_{\mathrm{B}}} - \sum_i \frac{\mu_i}{T_{\mathrm{B}}} \vec{J}_i \tag{29}$$

$$\sigma_{\mathrm{le}}^s = -\vec{q}_{\mathrm{B}} \cdot \frac{\vec{\nabla} T_{\mathrm{B}}}{T_{\mathrm{B}}^2} - \sum_i \vec{J}_i \cdot \vec{\nabla} \left(\frac{\mu_i}{T_{\mathrm{B}}} \right) + \frac{v_{\mathrm{ch}} A_{\mathrm{le}}}{T_{\mathrm{B}}} + \alpha_{\mathrm{A}} \frac{T_{\mathrm{A}} - T_{\mathrm{B}}}{T_{\mathrm{A}} T_{\mathrm{B}}}. \tag{30}$$

According to the Curie 'principle' [15, 44], fluxes and forces of different tensorial order do not couple. Thus we consider the following form for the so-called constitutive or phenomenological equations:

$$\vec{q}_{\mathrm{B}} = -L_q \frac{\vec{\nabla} T_{\mathrm{B}}}{T_{\mathrm{B}}^2} - \sum_i M_{qi} \vec{\nabla} \left(\frac{\mu_i}{T_{\mathrm{B}}} \right) \tag{31}$$

$$\vec{J}_i = -L_i \vec{\nabla} \left(\frac{\mu_i}{T_{\mathrm{B}}} \right) - \sum_{j \neq i} M_{ij} \vec{\nabla} \left(\frac{\mu_j}{T_{\mathrm{B}}} \right) - M_{iq} \frac{\vec{\nabla} T_{\mathrm{B}}}{T_{\mathrm{B}}^2} \tag{32}$$

$$v_{\mathrm{ch}} = \varkappa A_{\mathrm{le}} + M_{v\alpha} (T_{\mathrm{A}} - T_{\mathrm{B}}) \tag{33}$$

$$\alpha_{\mathrm{A}} = \alpha (T_{\mathrm{A}} - T_{\mathrm{B}}) + M_{\alpha v} A_{\mathrm{le}}. \tag{34}$$

The second law of thermodynamics requires that $\sigma_{\mathrm{le}}^s \geqslant 0$. This implies that $\lambda_{\mathrm{B}} \equiv L_q / T_{\mathrm{B}}^2 \geqslant 0$ (λ_{B} is the thermal conductivity of component B), $L_i \geqslant 0$, $\varkappa \geqslant 0$ and $\alpha \geqslant 0$. Additional restrictions for the cross coefficients M_{qi}, M_{ij}, $M_{v\alpha}$, etc, can be easily derived in the usual way [15], but they are not necessary for the purposes of this paper. Let us, however, mention that the Onsager symmetry relations [15] are in this case $M_{qi} = M_{ij} = M_{ji}$ and $M_{\alpha v} = M_{v\alpha}$. Equation (31) may be written as

$$\vec{q}_{\mathrm{B}} = -\lambda_{B\mathrm{eff}} \vec{\nabla} T_{\mathrm{B}} - \sum_j D_{qj} \vec{\nabla} \hat{c}_j \tag{35}$$

where $\lambda_{B\mathrm{eff}} \equiv \lambda_{\mathrm{B}} - \sum_i (M_{qi} \mu_i) / T_{\mathrm{B}}^2 + \sum_i (M_{qi} \partial \mu_i / \partial T_{\mathrm{B}}) / T_{\mathrm{B}}$ is an effective thermal conductivity, and $D_{qj} \equiv \sum_i (M_{qi} \partial \mu_i / \partial \hat{c}_j) / T_{\mathrm{B}}$ are thermodiffusion coefficients. If the cross terms were neglected, equations (32) and (35) would become the Fourier and Fick laws, respectively [14, 15]. Equation (34) describes the equilibration of temperatures between the components. On the other hand, equation (33) without the cross term has previously been discussed in detail [21, 38] and is unrealistic except if the local-equilibrium affinity A_{le} is small enough (see [21] and references therein). However, if cross terms can be neglected equation (33) is not relevant in order to analyse the propagation of thermal wavefronts. This will be performed in section 3, and compared to experiment in section 4, by means of equations (34) and (35).

In this section we have generalized the usual irreversible thermodynamical analysis of several-temperature systems [13] to the case in which there is a chemical reaction with energy

source terms F_i. In contrast to the usual CIT approach [13], we have taken such chemical source terms into account because, as we shall see (section 3), they are necessary for the propagation of thermal wavefronts.

2.2. EIT

As noted by Landau and Lifshitz [45, pp 194–5], the classical theory of heat conduction (based on Fourier's law, equation (31)) predicts that the effect of any thermal perturbation is propagated instantaneously through all space. This is why extensions of the Fourier law, avoiding this result, have been proposed and used for a long time. They can be derived from EIT [15–20]. We will apply this approach to reacting systems with several temperatures, by extending the CIT model presented in section 2.1. Since the procedure is similar to that applied to radiation–matter systems with two temperatures (section 4 in [36]), it will be sufficient to give the main steps.

The starting point in EIT is to consider that the specific entropy depends on the heat and diffusion fluxes in addition to the classical variables of CIT [15–20]. Thus in this framework we may assume that near equilibrium equation (15) is generalized into

$$\frac{\mathrm{d}s}{\mathrm{d}t} = \sum_i \frac{1}{\theta_i} \frac{\mathrm{d}\hat{u}_i}{\mathrm{d}t} - \sum_i \frac{\eta_i}{\theta_i} \frac{\mathrm{d}\hat{c}_i}{\mathrm{d}t} - \frac{\gamma_B(\hat{u}_B)}{T_B \rho} \vec{q}_B \cdot \frac{\mathrm{d}\vec{q}_B}{\mathrm{d}t} - \sum_i \frac{\delta_i(\hat{u}_i)}{T_i \rho} \vec{J}_i \cdot \frac{\mathrm{d}\vec{J}_i}{\mathrm{d}t} \quad (36)$$

where we have introduced the nonequilibrium thermodynamical temperatures θ_i and chemical potentials η_i of the components, as well as the quantities $\gamma_B(\hat{u}_B)$ and $\delta_i(\hat{u}_i)$, as

$$\frac{1}{\theta_i} \equiv \frac{\partial s}{\partial \hat{u}_i} \quad (37)$$

$$\eta_i \equiv -\theta_i \frac{\partial s}{\partial \hat{c}_i} \quad (38)$$

$$\frac{\gamma_B(\hat{u}_B)}{T_B \rho} \vec{q}_B \equiv -\frac{\partial s}{\partial \vec{q}_B} \quad (39)$$

$$\frac{\delta_i(\hat{u}_i)}{T_i \rho} \vec{J}_i \equiv -\frac{\partial s}{\partial \vec{J}_i}. \quad (40)$$

These equations are analogous to the corresponding nonequilibrium ones for radiation–matter systems at different temperatures, introduced in section 4 of [36].

We recall that, for simplicity, we have assumed a two-temperature system: the inert component A has its own temperature and the reacting components B, C and D have another one (so $\theta_B = \theta_C = \theta_D$, in analogy to equation (3)). Now because the entropy density must be an exact differential, we can require the second cross derivatives to be independent of the order of derivation ($\frac{\partial^2 s}{\partial \vec{q}_B \partial \hat{u}_i} = \frac{\partial^2 s}{\partial \hat{u}_i \partial \vec{q}_B}$ etc). This yields, in particular

$$\frac{1}{\theta_B} = \frac{1}{T_B} - \frac{\vec{q}_B \cdot \vec{q}_B}{2\rho} \frac{\partial}{\partial \hat{u}_B} \left(\frac{\gamma_B}{T_B} \right) - \sum_i \frac{\vec{J}_i \cdot \vec{J}_i}{2\rho} \frac{\partial}{\partial \hat{u}_i} \left(\frac{\delta_i}{T_B} \right) \quad (41)$$

$$\theta_A = T_A. \quad (42)$$

As in the previous section, we now use in equation (36) the balance equation for $\hat{u}_B$ (equation (20)) and the corresponding ones for the other species, as well as equations (6), (7), (11) and (12). This yields

$$\rho \frac{\mathrm{d}s}{\mathrm{d}t} = -\frac{\vec{\nabla} \cdot \vec{q}_B}{\theta_B} + \alpha_A \left(\frac{1}{\theta_B} - \frac{1}{\theta_A} \right) - \frac{\rho}{\theta_B} \left(\eta_B \frac{\mathrm{d}\hat{c}_B}{\mathrm{d}t} + \eta_C \frac{\mathrm{d}\hat{c}_C}{\mathrm{d}t} + \eta_D \frac{\mathrm{d}\hat{c}_D}{\mathrm{d}t} \right)$$

$$-\frac{\gamma_{\mathrm{B}}(\hat{u}_{\mathrm{B}})}{T_{\mathrm{B}}}\vec{q}_{\mathrm{B}}\cdot\frac{\mathrm{d}\vec{q}_{\mathrm{B}}}{\mathrm{d}t}-\sum_i\frac{\delta_i(\hat{u}_i)}{T_{\mathrm{B}}}\vec{J}_i\cdot\frac{\mathrm{d}\vec{J}_i}{\mathrm{d}t} \tag{43}$$

which generalizes equation (21). Making use of equations (23)–(26), the third term on the RHS may be rewritten in terms of the generalized chemical affinity of the reaction (2), which we define as

$$A\equiv\eta_{\mathrm{B}}m_{\mathrm{B}}\nu_{\mathrm{B}}+\eta_{\mathrm{C}}m_{\mathrm{C}}\nu_{\mathrm{C}}-\eta_{\mathrm{D}}m_{\mathrm{D}}\nu_{\mathrm{D}}. \tag{44}$$

This yields

$$\rho\frac{\mathrm{d}s}{\mathrm{d}t}=-\frac{\vec{\nabla}\cdot\vec{q}_{\mathrm{B}}}{\theta_{\mathrm{B}}}+\alpha_{\mathrm{A}}\left(\frac{1}{\theta_{\mathrm{B}}}-\frac{1}{\theta_{\mathrm{A}}}\right)+\sum_i\frac{\eta_i}{\theta_{\mathrm{B}}}\vec{\nabla}\cdot\vec{J}_i+\frac{\nu_{\mathrm{ch}}A}{\theta_{\mathrm{B}}}$$
$$-\frac{\gamma_{\mathrm{B}}(\hat{u}_{\mathrm{B}})}{T_{\mathrm{B}}}\vec{q}_{\mathrm{B}}\cdot\frac{\mathrm{d}\vec{q}_{\mathrm{B}}}{\mathrm{d}t}-\sum_i\frac{\delta_i(\hat{u}_i)}{T_{\mathrm{B}}}\vec{J}_i\cdot\frac{\mathrm{d}\vec{J}_i}{\mathrm{d}t}. \tag{45}$$

Comparison with the general law of balance of entropy, as in the previous section 2.1, now leads to the following identifications for the entropy flux $\vec{J}^s$ and entropy production rate σ^s:

$$\vec{J}^s=\frac{\vec{q}_{\mathrm{B}}}{\theta_{\mathrm{B}}}-\sum_i\frac{\eta_i}{\theta_{\mathrm{B}}}\vec{J}_i \tag{46}$$

$$\sigma^s=-\vec{q}_{\mathrm{B}}\cdot\left(\frac{\vec{\nabla}\theta_{\mathrm{B}}}{\theta_{\mathrm{B}}^2}+\frac{\gamma_{\mathrm{B}}(\hat{u}_{\mathrm{B}})}{T_{\mathrm{B}}}\frac{\mathrm{d}\vec{q}_{\mathrm{B}}}{\mathrm{d}t}\right)-\sum_i\vec{J}_i\cdot\left(\vec{\nabla}\left(\frac{\eta_i}{\theta_{\mathrm{B}}}\right)+\frac{\delta_i(\hat{u}_i)}{T_{\mathrm{B}}}\frac{\mathrm{d}\vec{J}_i}{\mathrm{d}t}\right)$$
$$+\frac{\nu_{\mathrm{ch}}A}{\theta_{\mathrm{B}}}+\alpha_{\mathrm{A}}\frac{\theta_{\mathrm{A}}-\theta_{\mathrm{B}}}{\theta_{\mathrm{A}}\theta_{\mathrm{B}}}. \tag{47}$$

This suggests, in the spirit of EIT [15], consideration of evolution equations with additional terms containing the time derivatives of the fluxes. Thus we generalize equations (31)–(34) by including terms in $\mathrm{d}\vec{q}_{\mathrm{B}}/\mathrm{d}t$ and $\mathrm{d}\vec{J}_i/\mathrm{d}t$,

$$\vec{q}_{\mathrm{B}}=-\lambda_{\mathrm{B}}\left(\vec{\nabla}\theta_{\mathrm{B}}+\gamma_{\mathrm{B}}(\hat{u}_{\mathrm{B}})T_{\mathrm{B}}\frac{\mathrm{d}\vec{q}_{\mathrm{B}}}{\mathrm{d}t}\right)-\sum_i N_{qi}\vec{J}_i \tag{48}$$

$$\vec{J}_i=-L_i\left(\vec{\nabla}\left(\frac{\eta_i}{\theta_{\mathrm{B}}}\right)+\frac{\delta_i(\hat{u}_i)}{T_{\mathrm{B}}}\frac{\mathrm{d}\vec{J}_i}{\mathrm{d}t}\right)-\sum_{j\neq i}N_{ij}\vec{J}_j-N_{iq}\vec{q}_{\mathrm{B}} \tag{49}$$

$$\nu_{\mathrm{ch}}=\varkappa A+M_{\nu\alpha}(\theta_{\mathrm{A}}-\theta_{\mathrm{B}}) \tag{50}$$

$$\alpha_{\mathrm{A}}=\alpha(\theta_{\mathrm{A}}-\theta_{\mathrm{B}})+M_{\alpha\nu}A \tag{51}$$

and the second law ($\sigma^s\geqslant 0$) implies that $\lambda_{\mathrm{B}}\geqslant 0$, $L_i\geqslant 0$, $\varkappa\geqslant 0$ and $\alpha\geqslant 0$. One could of course include terms containing the time derivatives of ν_{ch} and α_{A} in equations (50) and (51) (see [21]) but there is as yet no experimental evidence for such terms (moreover, they would make calculations extremely cumbersome). Defining, analogously to what has been done in equation (35), $\lambda_{\mathrm{Beff}}\equiv\lambda_{\mathrm{B}}+\sum_i(N_{qi}L_i\eta_i)/\theta_{\mathrm{B}}^2-\sum_i(N_{qi}L_i\partial\eta_i/\partial\theta_{\mathrm{B}})/\theta_{\mathrm{B}}$ and $D_{qj}\equiv\sum_i(N_{qi}L_i\partial\eta_i/\partial\hat{c}_j)/\theta_{\mathrm{B}}$, and also the thermal relaxation time of component B as

$$\tau_{\mathrm{B}}\equiv\lambda_{\mathrm{B}}\gamma_{\mathrm{B}}(\hat{u}_{\mathrm{B}})T_{\mathrm{B}} \tag{52}$$

and neglecting higher-order terms, equation (48) becomes

$$\vec{q}_{\mathrm{B}}+\tau_{\mathrm{B}}\frac{\mathrm{d}\vec{q}_{\mathrm{B}}}{\mathrm{d}t}=-\lambda_{\mathrm{Beff}}\vec{\nabla}\theta_{\mathrm{B}}-\sum_j D_{qj}\vec{\nabla}\hat{c}_j. \tag{53}$$

This is nothing but the Maxwell–Cattaneo equation [15], here derived for a single component B of the mixture, with the additional thermodiffusion terms. Equations (51) and (53), which

generalize (31) and (34), will be used in section 3.2 to analyse the propagation of thermal wavefronts in the EIT approach. The remaining equations are not necessary for this purpose, and this is why we have not computed the nonequilibrium chemical potentials η_i explicitly. Let us however mention that equation (49) is a relaxational equation for diffusion, which has been previously considered (see equation (10.6) in [15]) and here includes an additional thermodiffusion term.

It is worthwhile to observe that equations (51) and (53) without cross terms have been considered by Sobolev [28], who did not, however, distinguish between the nonequilibrium temperature θ_B and the local-equilibrium one T_B. The reason lies in the fact that Sobolev did not carry out a first-principles EIT development such as the one presented here. This point is interesting because we have shown that both temperatures are different (see equation (41)), and, since it is the nonequilibrium temperature θ_B that appears in equation (51), the thermal exchange between components is driven by the difference $\theta_A - \theta_B$ rather than $T_A - T_B$. This is not surprising, since an analogous result has been derived for the much simpler case of radiation–matter systems (see equation (35) in [36]), but the corresponding analysis for multi-temperature matter systems had not been presented before in the literature. It gives a thermodynamical, sound foundation to the application presented in section 3.2, where the generalized temperatures θ_i will be used (instead of T_i), in agreement with the results derived above. Besides this, our new result that $\theta_A - \theta_B$ (instead of $T_A - T_B$) is the driving force of energy transfer (in nonequilibrium multitemperature systems) should also be useful concerning the debate on the correct definition of temperature outside LTE [46].

3. Thermal wavefronts

In this section we apply the models presented in section 2 to the propagation of reaction–conduction wavefronts. This will allow us to generalize some classical results to the case in which heat losses are important (section 3.1) and to analyse the consequences of the finite propagation speed of thermal signals (section 3.2).

In order to analyse temperature changes related to the proceeding of, say, an exothermic chemical reaction, it will be useful to write the mean energy E_i of a molecule of species i, already considered in equations (5)–(7), as

$$E_i = E_{ki} + E_{pi} \tag{54}$$

where E_{ki} stands for the mean kinetic (i.e. thermal) energy, and E_{pi} for the mean potential (i.e. electronic) energy of a molecule of species i. The heat of the chemical reaction (2) is [26]

$$Q \equiv \nu_D E_{kD} - \nu_B E_{kB} - \nu_C E_{kC} = \nu_B E_{pB} + \nu_C E_{pC} - \nu_D E_{pD} \tag{55}$$

where use has been made of the conservation of energy (equation (7)). We shall from now on consider an exothermal chemical reaction, i.e. $Q > 0$. Note that when using the second law of thermodynamics (section 2) we have applied the total energies E_i, thereby taking into account the entropy production due to all of the processes in the system. By contrast, now we are interested in the evolution of temperatures. This will be related to the reaction heat Q, which is in turn linked to the kinetic energies E_{ki}. Therefore, it will be useful to define the kinetic energy per unit mass of species i as u_{ki}. Then we have

$$\frac{\partial}{\partial t}(\rho_B u_{kB}) = -\vec{\nabla} \cdot \vec{q}_B - \nu_B \nu_{ch} E_{kB} + \alpha_{AB} \tag{56}$$

$$\frac{\partial}{\partial t}(\rho_C u_{kC}) = -\nu_C \nu_{ch} E_{kC} + \alpha_{AC} \tag{57}$$

$$\frac{\partial}{\partial t}(\rho_B u_{kD}) = \nu_D \nu_{ch} E_{kD} + \alpha_{AD} \tag{58}$$

which are analogous to equations (5), (9) and (10), with the difference that now the kinetic specific and mean energies (u_{ki} and E_{ki}, respectively) appear instead of the total ones (u_i and E_i). The evolution equation for the temperature T_B of the reacting species can be now derived. By defining the density ρ_r and specific internal energy u_{kr} of the reactive subsystem as

$$\rho_r \equiv \rho_B + \rho_C + \rho_D \tag{59}$$

$$\rho_r u_{kr} \equiv \rho_B u_{kB} + \rho_C u_{kC} + \rho_D u_{kD} \tag{60}$$

from equations (56)–(60) we obtain

$$\rho_r c_r \frac{\partial T_B}{\partial t} = -u_{kr} \frac{\partial \rho_r}{\partial t} + \frac{\partial}{\partial t}(\rho_B u_{kB}) + \frac{\partial}{\partial t}(\rho_C u_{kC}) + \frac{\partial}{\partial t}(\rho_D u_{kD})$$

$$= -u_{kr} \frac{\partial \rho_r}{\partial t} - \vec{\nabla} \cdot \vec{q}_B + v_{ch}(-\nu_B E_{kB} - \nu_C E_{kC} + \nu_D E_{kD}) + \alpha_A \tag{61}$$

where $c_r \equiv (\rho_B c_B + \rho_C c_C + \rho_D c_D)/\rho_r$, with c_i the specific heat of component i, and we have recalled that $\alpha_A \equiv \alpha_{AB} + \alpha_{AC} + \alpha_{AD}$. By making use of the mass balance equations (23)–(26), the definitions $\vec{J}_i \equiv \rho_i(\vec{v}_i - \vec{v})$ and $\rho \vec{v} \equiv \sum_i \rho_i \vec{v}_i$ (in this paper we have assumed $\vec{v} = 0$, but $\sum_i \vec{J}_i = 0$ holds in general), and the conservation of mass in the chemical reaction (2) (i.e. $\nu_B m_B + \nu_C m_C = \nu_D m_D$), the first term in the RHS of equation (61) is easily seen to vanish. Use of equation (55) finally yields

$$\rho_r c_r \frac{\partial T_B}{\partial t} = -\vec{\nabla} \cdot \vec{q}_B + v_{ch} Q + \alpha_A \tag{62}$$

so the reaction heat Q increases T_B, as it should. T_B is the temperature of the reacting species B, C and D, which lose energy to the inert component A (the last term in equation (62)).

3.1. CIT

From equation (62) and the CIT equations (34) and (35) we obtain the evolution equation for the temperature T_B as

$$\rho_r c_r \frac{\partial T_B}{\partial t} = \lambda_{Beff} \nabla^2 T_B + \sum_i D_{qi} \nabla^2 \hat{c}_i + Q v_{ch}(T_B) + \alpha(T_A - T_B) + M_{\alpha v} A_{le}. \tag{63}$$

The last term describes a cross effect between chemical reaction and temperature equilibration, and is likely to have small relevance within CIT (it will be dropped when comparing with experiment in section 4). However, it may be important in special applications, e.g. as compared with the additional terms arising from EIT (section 3.2), so let us include it here for completeness. Using equation (33) and neglecting higher-order terms,

$$\rho_r c_r \frac{\partial T_B}{\partial t} = \lambda_{Beff} \nabla^2 T_B + \sum_i D_{qi} \nabla^2 \hat{c}_i + Q v_{ch}(T_B) + \alpha(T_A - T_B) + \frac{M_{\alpha v}}{\varkappa} v_{ch}(T_B). \tag{64}$$

In general, equation (63) is coupled to the evolution equation for T_A, which can be obtained by using the analogue to equations (56)–(58) for component A, namely $\partial(\rho_A u_{kA})/\partial t = -\alpha_A$, equations (33) and (34) and neglecting higher-order terms as above,

$$\rho_A c_A \frac{\partial T_A}{\partial t} = -\alpha(T_A - T_B) - \frac{M_{\alpha v}}{\varkappa} v_{ch}(T_B) \tag{65}$$

where c_A is the specific heat of component A. Equation (65) has the typical form used in the description of energy equilibration processes in mixtures (see, e.g., [47, 48]), with an additional cross term. Equations (64) and (65) are analogous to the Lotka–Volterra equations used in population dynamics (e.g. predator–prey and parasite–host systems) [29] and to the Ginzburg–Landau equations used in the analysis of front propagation in superconductors [49],

with an additional cross term. As in those systems, the evolution of the field variables (T_B and T_A in our case) are coupled, but in order to analyse the propagation of wavefronts we can proceed as follows. Consider, for example, a system in which at $t = 0$ all components have the same temperature ($T_B = T_A$). Then, some of the components are heated in a localized region of the system, so that T_B is locally increased. One example is laser-heating of metals, where electrons absorb the radiation energy (whereas the heat absorbed directly by the lattice is negligible) [7]. Another example is a locally activated chemical reaction such as (2) in the presence of a colder (or hotter), nonreacting component A. Heat conduction (the flux $\vec{q}_B$) will raise the temperature T_B in surrounding regions (the first term in the RHS of equation (63)), which will in turn speed up the chemical reaction (2). This will affect the evolution of T_B (the third term in the RHS of equation (63)), i.e. we have a joint effect of conduction and reaction (plus that arising from the energy transfer to component A, see the fourth term in the RHS of equation (63), and the cross effects described by the additional terms in equation (63)). In such an instance, we expect intuitively that a thermal wavefront will propagate into the region of the system where $T_B \simeq T_A$. For simplicity we consider a system in which all quantities depend on a single coordinate x, and assume that the temperature dependence of the parameters λ_r, α and c_r in equation (63) can be neglected in the range of temperatures considered (this is the usual approach in the study of thermal wavefront propagation [26]). In order to find out wavefront solutions moving with velocity v, we change to a frame moving with the wavefront by introducing the variable

$$z = x - vt \tag{66}$$

so that equation (63) becomes a single-variable differential equation,

$$-\rho_r c_r v \frac{dT_B}{dz} = \lambda_{Beff} \frac{d^2 T_B}{dz^2} + \sum_i D_{qi} \frac{d^2 \hat{c}_i}{dz^2} + \left(Q + \frac{M_{\alpha v}}{\varkappa} \right) v_{ch}(T_B) + \alpha(T_A - T_B). \tag{67}$$

We will apply the linearization method, which has been successfully used for reaction–diffusion systems (the temperatures in equations (63) and (65) are then replaced by the corresponding particle densities, and near the wavefront edge one has $n_A \simeq n_{A0}$ and $n_B \simeq n_{B0} + \varepsilon$, where n_{A0} and n_{B0} are the initial particle densities for the preexisting and incoming species, respectively, and ε is a perturbation [29,34]). In our case, near the wavefront edge the heat flux $\vec{q}_B$ will lead to an increase in the temperature of component B, which in the first-order approximation may be analogously written as $T_B \simeq T + \varepsilon$, where ε is a perturbation, whereas since $\vec{q}_A \simeq 0$ we will analogously have $T_A \simeq T$. Here T is the initial temperature, shared by all components before the arrival of the thermal front. The increase ε in T_B (due to the heat flux $\vec{q}_B$) will thereafter speed up the chemical reaction, changing the initial concentrations $\hat{c}_{i0}$. Thus, it is reasonable to linearize equation (67) under the ansatz $T_B \simeq T + \varepsilon$, $T_A \simeq T$ and $c_i \simeq \hat{c}_{i0}$, in complete analogy to the well established approach to reaction–diffusion explained above. In this way we obtain†

$$-\rho_r c_r v \frac{d\varepsilon}{dz} = \lambda_{Beff} \frac{d^2 \varepsilon}{dz^2} + \left(Q + \frac{M_{\alpha v}}{\varkappa} \right) \left. \frac{\partial v_{ch}}{\partial T_B} \right|_T \varepsilon - \alpha \varepsilon. \tag{68}$$

† In general, the reactive term in equation (68) is $(Q + \frac{M_{\alpha v}}{\varkappa})(v_{ch}|_T + \frac{\partial v_{ch}}{\partial T_B}|_T \varepsilon)$. However, the first term inside the second parentheses can be neglected for flames with an essentially isothermal region, the so-called pyrolysis zone, which is observed in the experimental temperature profiles of flames over cellulosic fuels (see e.g. figure 3 in [50] and comments therein). In a frame moving with the flame front, the system variables are homogeneous within the pyrolysis region so equation (67) yields $(Q + \frac{M_{\alpha v}}{\varkappa})v_{ch}(T_B) + \alpha(T_A - T_B) = 0$, which means that heat losses compensate the exothermic reaction in the pyrolysis zone. In this zone, $\varepsilon \equiv T_B - T \simeq 0$, with T the so-called pyrolysis temperature [50], and equation (68) with inclusion of the whole reactive term yields precisely $v_{ch}|_T \simeq 0$ in the linear approximation. This is analogous to the corresponding approximation used in the source term of reaction–diffusion systems (e.g., the use of $f(0) = 0$ in [34]), and is shown to yield good agreement with experiment for flame speed over cellulosic fuels in section 4 in this paper. It can be easily applied to radiative losses also; see the note in this paper.

Solutions with the form $\varepsilon(z) \sim e^{\mu z}$ lead to the characteristic equation

$$\lambda_{\text{Beff}} \mu^2 + \rho_r c_r v \mu + \left(Q + \frac{M_{\alpha v}}{\varkappa} \right) \left. \frac{\partial v_{\text{ch}}}{\partial T_{\text{B}}} \right|_T - \alpha = 0. \tag{69}$$

Solving this equation for μ and requiring that $\mu \in R$ we find that the minimum propagation velocity of the thermal wavefront is

$$v = \frac{2\sqrt{\lambda_{\text{Beff}}}}{\rho_r c_r} \sqrt{\left(Q + \frac{M_{\alpha v}}{\varkappa} \right) \left. \frac{\partial v_{\text{ch}}}{\partial T_{\text{B}}} \right|_T - \alpha}. \tag{70}$$

If cross effects can be neglected ($M_{\alpha v} \simeq 0$, see the text below equation (63), and $M_{qi} \simeq 0$, so that $\lambda_{\text{Beff}} \simeq \lambda_{\text{B}}$ and $D_{qi} \simeq 0$, see below equation (51)), we obtain

$$v = \frac{2\sqrt{\lambda_{\text{B}}}}{\rho_r c_r} \sqrt{Q \left. \frac{\partial v_{\text{ch}}}{\partial T_{\text{B}}} \right|_T - \alpha}. \tag{71}$$

In section 4 the predictions of this equation will be compared with experimental results.

Note that $\tau_r \equiv \rho_r c_r / (Q \frac{\partial v_{\text{ch}}}{\partial T_{\text{B}}}|_T)$ and $\tau_e \equiv \rho_r c_r / \alpha$ have units of time. They may be seen as characteristic time scales of the chemical reaction and the temperature equilibration process, respectively. Therefore, according to equation (71) the order of magnitude of the propagation speed is

$$v \sim \sqrt{\frac{\chi_{\text{B}}}{\tau_r} - \frac{\chi_{\text{B}}}{\tau_e}} \tag{72}$$

with $\chi_{\text{B}} \equiv \frac{\lambda_{\text{B}}}{\rho_r c_r}$ the thermal diffusivity of the reactive subsystem, due to the conduction of heat by component B. In the absence of energy transfer to the nonreacting component A ($\alpha = 0$), this becomes

$$v \sim \sqrt{\frac{\chi_{\text{B}}}{\tau_r}} \tag{73}$$

which agrees with the order-of-magnitude estimation performed in a different way by Landau and Lifshitz [45, p 475], for the single-temperature case ($\alpha = 0$).

Below we will also compare our results to some analogous ones for non-conducting systems and to those from the detailed analysis of combustion waves due to Zeldovich *et al* [26]. Before doing so, we may note that the model presented is valid provided that $Q \frac{\partial v_{\text{ch}}}{\partial T_{\text{B}}}|_T > \alpha$; otherwise equation (71) breaks down and there are no wavefront solutions for the field T_{B}. This is due to the fact that in such an instance the effect of the energy transfer to the inert species A dominates the dynamics: the temperatures T_{A} and T_{B} become equilibrated in a shorter timescale than that of the reaction, i.e. we have $\tau_e > \tau_r$ (this follows directly from the definitions of these quantities below equation (71)). This means that the approximation $T_{\text{A}} \simeq T$, applied above, breaks down even in the leading edge of the front ($T_{\text{B}} \simeq T + \varepsilon$).

Let us now introduce the following dimensionless variables:

$$t^* = \kappa t \tag{74}$$

$$\alpha^* = \frac{\alpha}{\kappa \rho_r c_r} \tag{75}$$

$$x^* = \sqrt{\frac{\kappa \rho_r c_r}{\lambda_{\text{B}}}} x \tag{76}$$

where κ is the inverse of a characteristic time for the chemical reaction (e.g. $1/\tau_r$, with τ_r defined above). Then

$$v^* = \sqrt{\frac{\rho_r c_r}{\lambda_{\text{B}} \kappa}} v \tag{77}$$

and after introducing $F^* = Qv_{ch}/(\kappa\rho_r c_r)$—which has units of temperature, equation (71) can be written in dimensionless form,

$$v^* = 2\sqrt{\left.\frac{\partial F^*}{\partial T_B}\right|_T - \alpha^*}. \tag{78}$$

This equation is the thermal analogue to equation (12.10) in [29], which analyses wavefronts in diffusive predator–prey systems (instead of conductive systems, which are the ones considered here). It is also analogous to equation (7) in [49], which applies to the propagation of domain walls in superconductors. In the special case $\alpha^* = 0$, equation (78) is nothing but the thermal analogue to the well known Fisher–Piskunov minimal propagation velocity for reaction–diffusion fronts [26, 29].

In order to compare equation (78) to Zeldovich's results, let us consider a combustion process for a bimolecular chemical reaction ($\nu_B = \nu_C = 1$ in equation (2)) with Arrhenius kinetics [25, 26],

$$v_{ch} = \tilde{A}\exp\left[-\frac{E_a}{kT_B}\right]n_B n_C \tag{79}$$

where the temperature dependence of the pre-exponential factor $\tilde{A}$ can, for practical purposes, be ignored [25, 26], E_a is the activation energy and k is Boltzmann's constant. As explained above, and is applied in combustion theory [26], in thermal fronts heat is transferred by conduction, which afterwards activates the chemical reaction; thus we may ignore the perturbations in the concentrations with respect to their initial values n_{B0} and n_{C0}. Then, use of equation (79) into (78) yields

$$v^* = 2\sqrt{A^* e^{-E_a/kT} - \alpha^*} \tag{80}$$

where $A^* = \tilde{A}Qn_{B0}\,n_{C0}E_a/(\kappa\rho_r c_r kT^2)$.

For $\alpha^* = 0$, equation (80) reduces to

$$v^* \sim e^{-E_a/2kT} \tag{81}$$

which is the classical result due to Zeldovich for the minimal propagation speed of combustion fronts (see equations (4.21) and (4.41) in [26]). Experimentally it is observed that, after an initial transient, the front evolves according to this minimal speed [26]. Equation (80) generalizes Zeldovich's result.

Below equation (34) we have seen that the second law of thermodynamics implies that $\alpha^* > 0$. It is thus seen from equation (80) that the presence of this parameter lowers the propagation velocity of the thermal front, as was to be expected intuitively since it corresponds to a heat loss due to the presence of the nonreacting component A (see the term $\alpha(T_A - T_B)$ in equation (63)). In figure 1 we illustrate this effect for some values of E_a/kT in the typical range of combustion reactions [26]. It is worthwhile to observe that for this range we have $E_a/kT > 12$, so additional nonequilibrium effects related to the reverse reaction can be neglected and the Arrhenius equation in its simplest form, namely equation (79), can be applied [10]. The dashed curve in figure 1 is the classical result (figure 1.30 in [26]), and the other curves correspond to its generalization to several-temperature systems. The predicted decrease of wavefront propagation shown in figure 1 follows from equation (80).

In the next section, the previous results will be generalized by taking into account an additional effect, namely that resulting from the finite speed of thermal signals.

3.2. EIT

The time-delayed equation (53) describes a different heat conduction regime than that corresponding to the classical, Fourier-type law (35). Time-delayed equations have been
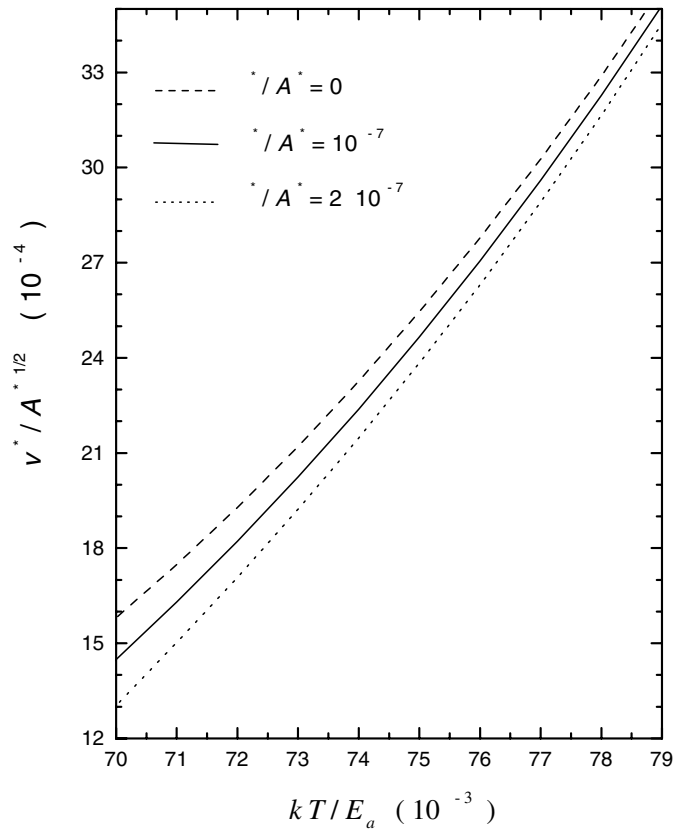
Figure 1. Comparative plot of the predictions for the dimensionless speed of combustion wavefronts as a function of the dimensionless temperature (see equation (80)). The dashed curve ($\alpha* = 0$) is the curve due to Zeldovich (see figure 1.30 in [26]). When there is a heat loss mechanism at work ($\alpha* \neq 0$), the propagation speed is decreased.

widely studied for single-temperature systems and are known to avoid the problem (mentioned at the beginning of section 2.2) of the infinite speed of thermal signals [15]. Here we will analyse the consequences on the propagation of thermal wavefronts. Use of the EIT equations (51) and (53) in the energy conservation equation (62) yields the following temperature evolution equation:

$$\rho_r c_r \frac{\partial}{\partial t}\left(\theta_B + \tau_B \frac{\partial \theta_B}{\partial t}\right) = \lambda_{B\text{eff}}\nabla^2\theta_B + \sum_i D_{qi}\nabla^2\hat{c}_i + \left(Q + \frac{M_{\alpha v}}{\varkappa}\right)\left(v_{\text{ch}} + \tau_B \frac{\partial v_{\text{ch}}}{\partial t}\right)$$

$$+\alpha\left[(\theta_A - \theta_B) + \tau_B \frac{\partial(\theta_A - \theta_B)}{\partial t}\right] \tag{82}$$

which reduces, as it should, to equation (64) in the infinite-speed limit for thermal signals (i.e. of vanishing delay time, $\tau_B \to 0$ [15]). Equation (82) is an extension of the well known telegrapher's equation because of the presence of the terms in v_{ch} and its time derivative (due to the chemical reaction) and $\alpha(\theta_A - \theta_B)$ and its time derivative (due to the relaxation of energy among the chemical species), as well as cross effects. By following exactly the same steps as in section 3.1, we obtain that equation (69) is generalized into

$$(\lambda_{B\text{eff}} - \tau_B \rho_r c_r v^2)\mu^2 + (\rho_r c_r - \tau_B \Lambda)v\mu + \Lambda = 0 \tag{83}$$

with $\Lambda \equiv (Q + \frac{M_{\alpha v}}{\varkappa})\frac{\partial v_{\text{ch}}}{\partial \theta_B}|_\theta - \alpha$.

Solving this equation for μ and requiring that $\mu \in R$ we find that the minimum velocity of the thermal wavefront is

$$v = \frac{2\sqrt{\lambda_{\text{Beff}}\Lambda}}{\rho_r c_r + \tau_{\text{B}}\Lambda}. \tag{84}$$

This result reduces, as it should, to equation (70) in the limit $\tau_{\text{B}} \to 0$. We see from equations (70) and (84) that, for a given value of the temperature read by a thermometer (θ in the case of equation (84) and T in the case of equation (70)), the effect of the delay time τ_{B} of heat conduction is to lower the speed of thermal wavefronts, as was to be expected intuitively.

4. Comparison with experiment

In the previous section we analysed the propagation speed of thermal wavefronts according to the CIT approach (section 3.1) and to the time-delayed, or EIT one (section 3.2). The latter approach may be of interest in the context of forest-fire models, in which a delay time connected to the ignition of a green tree close to a burning one is used [27]. However, this application requires a very detailed and lengthy analysis and will not be treated here. We will, instead, compare the predictions of the CIT approach (section 3.1) with experiment. Clearly, this is a necessary comparison before attempting the much more complicated problem of forest fires, in which many additional factors become important (e.g., the time delay mentioned above, the spatial heterogeneities linked to the mean distance among trees, the wind and slope effects, turbulence, etc).

We will not include cross terms, as usual in combustion studies. They are typically, if not always, neglected in the literature on combustion because it is reasonable to expect them to be negligible within the CIT approach (moreover, they cannot be evaluated from the experimental data available because the cross coefficients have not been measured for those systems for which we will compare with measured flame speeds).

As we have stressed, up to this point we have not assumed a specific heat loss mechanism. In this section we will consider one that often appears, namely radiative heat losses. In spite of the fact that, for the sake of clarity, we have often referred to an inert component responsible for heat losses, our formalism can be easily applied to radiation losses. Then, the heat loss term in the energy conservation equation (i.e. in our equations (62), (63), (65) and (67)) is simply $\alpha_{\text{A}} = 4a\sigma(T_{\text{A}}^4 - T_{\text{B}}^4)$ (instead of $\alpha_{\text{A}} = \alpha(T_{\text{A}} - T_{\text{B}})$), with a the mean absorption coefficient, σ the Stefan–Boltzmann constant and T_{A} the room temperature [51]. It has been previously stressed [52–57] that in this case the entropy production is not bilinear. This means that the linear relationship $\alpha_{\text{A}} = \alpha(T_{\text{A}} - T_{\text{B}})$ (see equation (34)) does not hold (except in the case $T_{\text{A}} \simeq T_{\text{B}}$). However, the wavefront analysis presented in section 3 can be applied, simply replacing the heat loss term in the equations mentioned above. It is also worth mentioning that there is thermodynamical consistency since it can be shown that $\sigma^s \geqslant 0$ for $\alpha_{\text{A}} = 4a\sigma(T_{\text{A}}^4 - T_{\text{B}}^4)$, as done originally by Planck [58] (see equation (6) in [52]). By following exactly the same steps as in section 3.1, we find that equation (68) is replaced by†

$$-\rho_r c_r v \frac{\text{d}\varepsilon}{\text{d}z} = \lambda_{\text{B}} \frac{\text{d}^2\varepsilon}{\text{d}z^2} + Q \left. \frac{\partial v_{\text{ch}}}{\partial T_{\text{B}}} \right|_T \varepsilon - 16a\sigma T^3 \varepsilon \tag{85}$$

---

† Since we neglect cross terms, equation (67) becomes $-\rho_r c_r v \frac{\text{d}T_{\text{B}}}{\text{d}z} = \lambda_{\text{B}} \frac{\text{d}^2 T_{\text{B}}}{\text{d}z^2} + Q v_{\text{ch}}(T_{\text{B}}) + 4a\sigma(T_{\text{A}}^4 - T_{\text{B}}^4)$. As in section 4.1, we set $T_{\text{B}} \simeq T + \varepsilon$, with T the pyrolysis temperature (see footnote on page 6963), whereas T_{A} is now the room temperature. Linearization yields $-\rho_r c_r v \frac{\text{d}\varepsilon}{\text{d}z} = \lambda_{\text{B}} \frac{\text{d}^2\varepsilon}{\text{d}z^2} + Q(v_{\text{ch}}|_T + \frac{\partial v_{\text{ch}}}{\partial T_{\text{B}}}|_T \varepsilon) + 4a\sigma(T_{\text{A}}^4 - T^4 - 4T^3\varepsilon) = 0$. The pyrolysis zone condition ($\varepsilon \simeq 0$, see footnote on page 6963) becomes $Q v_{\text{ch}}|_T + 4a\sigma(T_{\text{A}}^4 - T^4) = 0$. Subtracting these two equations we obtain equation (85).

and the propagation speed (71) becomes

$$v = \frac{2\sqrt{\lambda_B}}{\rho_r c_r} \sqrt{Q \left.\frac{\partial v_{ch}}{\partial T_B}\right|_T - 16 a\sigma T^3}. \tag{86}$$

We will compare with experimental data for flame spread over cellulosic fuels (paper and very thin wood samples). In these cases, combustion does not take place at room temperature but after evaporation and the release of combustible gases. The accepted temperature for the start of the exothermic reaction (fast pyrolysis) is $T = 280\,^{\circ}\mathrm{C} = 553$ K [59]†. We may note that this is well above the room temperature T_A, so in fact the approximation $\alpha_A = 4a\sigma(T_A^4 - T_B^4) \simeq -4a\sigma T_B^4$ can be applied. A global Arrhenius rate—similar to equation (79)—can be used [60],

$$v_{ch} = \tilde{A}\rho_{solid} \exp\left[-\frac{E_a}{RT_B}\right] \tag{87}$$

where ρ_{solid} is the fuel density, $R = 8.314$ J (mol K)$^{-1}$ and the recommended values for the kinetic parameters are $E_a = 3.1 \times 10^4$ cal mol^{-1} and $\tilde{A} = 7 \times 10^7$ s^{-1} [60].

With the Arrhenius rate law above, equation (86) becomes

$$v = \frac{2\sqrt{\lambda_B}}{\rho_r c_r} \sqrt{Q\frac{\rho_{solid} E_a \tilde{A}}{RT^2} - 16 a\sigma T^3} \tag{88}$$

and the global reaction heat is $Q = 2 \times 10^7$ J kg^{-1} [60]. In order to compare with experiment, we also need numerical values for the parameters λ_B, ρ_r, c_r, ρ_{solid} and a at $T = 553$ K. Since they are not available for the specific samples used in the experiments cited below, we shall use the recommended values for combustion studies of cellulosic fuels at $T = 553$ K. Note that this uncertainty in the values of the relevant parameters may be seen as additional reason to neglect cross terms, which will presumably have a lower effect. The recommended values are $\lambda_B = 0.15$ W (K m)$^{-1}$, $\rho_{solid} = 400$ kg m^{-3}, $\rho_r c_r = 8.97 \times 10^5$ J (kg K)$^{-1}$‡ and $a = 2.4$ m^{-1} [50]. Then, equation (88) yields a flame velocity of $v = 1.08 \times 10^{-4}$ m s^{-1}, which is of the same order of magnitude as that observed experimentally in [62] ($5.1(5) \times 10^{-4}$ m s^{-1}). Similar experimental results have been obtained by other authors§. Since the values of the parameters λ_B, c_{solid}, ρ_{solid} and a were not measured for the specific samples used, we consider that the order-of-magnitude agreement with experiment is satisfactory.

† A more recent summary of experimental data for both chemical kinetics and thermal parameters can be found in [60].
‡ λ_B is the thermal conductivity of the solid fuel since that of the gas is easily checked to be much lower ($\sim 10^{-2}$ W (K m)$^{-1}$ [61]) and would yield a slower flame speed. This means that heat conduction takes place mainly in the solid. On the other hand, according to [60], the average values of the density and specific heat are $\rho_{solid} = 400$ kg m^{-3} and $c_{solid} = 2241.6$ J (kg K)$^{-1}$. In our model (see the text below equation (61)), $\rho_r c_r = \rho_{solid} c_{solid} + \rho_{gas} c_{gas}$. Since, for example, $\rho_{O_2} c_{O_2} \sim 10^2$ J (kg K)$^{-1}$ [61], we have $\rho_r c_r \simeq \rho_{solid} c_{solid} = 8.97 \times 10^3$ J (kg K)$^{-1}$. Similarly $\rho_r \simeq \rho_{solid} = 400$ kg m^{-3} [60].
§ For the sake of completeness, we mention some additional experimental results. In [50], the relevant parameter values given by the authors are $Q = 11.76 \times 10^6$ J kg^{-1}, $\rho_r \simeq \rho_{solid} = 519$ kg m^{-3}, $a = 2.4$ m^{-1}, $E_a = 2.494 \times 10^5$ J mol^{-1}, $\tilde{A} = 7.8 \times 10^{16}$ s^{-1} and $T = 745$ K (see figure 3 in [50] and its discussion). The values of λ_B and c_r are not given in [50], so we have to estimate them again from the recommended values in [60] at this T, which are $\lambda_B = 0.22$ W (K m)$^{-1}$ and $c_r \simeq c_{solid} = 2984.0$ J (kg K)$^{-1}$. Then equation (88) yields $v = 5.5 \times 10^{-3}$ m s^{-1}, which is in reasonable agreement (concerning the order of magnitude) with the experimental value in [50], namely 4.4×10^{-3} m s^{-1}. We stress that a better agreement could be obtained if the values of λ_B and c_r were available for the specific filter paper used in these experiments. Similarly, Frey and T'ien [63] as well as LeVan [65] have measured $v \sim 10^{-3}$ m s^{-1} for the speed of flames over paper and over thin wood samples, respectively. Of course, our model is valid under the thin-fuel assumption, usual in solid combustion theory, since only in this case can the uni-dimensional approximation (i.e. the assumption that T depends only on x) be applied (see the text above equation (67)).

We now turn to the effect of radiative heat losses. If they were neglected, the front speed would be given by the approximation (see equation (88))

$$v_0 = \frac{2\sqrt{\lambda_{\mathrm{B}}}}{\rho_r c_r} \sqrt{Q \frac{\rho_{\mathrm{solid}} E_{\mathrm{a}} \tilde{A}}{RT^2}}. \tag{89}$$

For the same values of the parameters as above, this yields $v_0 = 1.09 \times 10^{-4}$ m s^{-1}, so the effect is 1%. Note that the value for a above corresponds to the absorption coefficient for paper samples [50], i.e. gas absorption is neglected, but, as Ronney and co-workers have recently stressed [64,66], in many cases the absorption coefficient is much higher because of the absorption by inert gases or mesoscopic particles present in the mixture. For example, in [66] the value $a = 26$ m^{-1} is considered. Then, the same values above for the other parameters yield a correction of 15%. This is illustrated in figure 2, where v, v_0 and the relative effect $(v_0 - v)/v$ (as a percentage) are plotted as functions of the absorption coefficient a for the same values of the other parameters as above. From figure 2, the importance of this possible effect is clear. It would of course be very interesting if experiments could be performed by varying the amount of inert gases [66] or absorbing mesoscopic particles [64] (i.e. the value of a) and comparing the observed speeds with the prediction in figure 2. We stress, however, that for such a comparison to be conclusive it would be necessary to measure not only the flame speed, but also all of the other parameters appearing in equation (88). From the comments and the literature survey presented above, this seems to be an interesting experimental problem, which does not seem to have been tackled in full detail and which, in our opinion, deserves attention.

The main point in our study is that, in contrast to solving a complex set of differential equations numerically (see, e.g., [50] and [66]), the front velocity can be evaluated readily from equation (88), provided of course that the values for the relevant parameters are available. Our approach is also completely different from activation-energy assymptotics, a method in which one assumes from the beginning a very high dimensionless activation energy (which we have not assumed), takes into account only higher-order derivatives in the evolution equations (which has not been done here) and keeps first-order terms in the inverse of the dimensionless activation energy [51,67–69].

Let us finally stress that in the case of mesoscopic particles (see [64] and references therein), when comparing with experiment the additional effect of the heat released due to collisions of the reacting gas molecules with the particles (equation (8) in this paper) should in general be included. We plan to deal with this topic in future work. Here we only mention that, using the approach presented, from equation (8) it is straightforward to see that

$$v = \frac{2\sqrt{\lambda_{\mathrm{B}}}}{\rho_r c_r} \sqrt{Q \frac{\rho_{\mathrm{solid}} E_{\mathrm{a}} \tilde{A}}{RT^2} - 16 a \sigma T^3 - \frac{\pi r^2}{\sqrt{\pi}} \frac{c_v P}{R} \left(\frac{8k}{m_{\mathrm{B}} T} \right)^{\frac{1}{2}} a_f n_{\mathrm{A}}} \tag{90}$$

which generalizes equation (88) because of the new term due to the collisions with the mesoscopic particles. We stress that, again, all of the parameters appearing in this equation (e.g., the number density n_{A} of mesoscopic particles) should be measured experimentally to make it possible to compare the order of magnitude of the flame speed predicted by this equation and that measured in experiments. Also, in this specific application the Knudsen accommodation factor a_f should ideally be measured by means of independent experiments (see [42]). Finally, a further effect that we plan to deal with in a future paper is radiative reabsorption by the inert particles. This will yield a net heat loss decrease and its role has been recently stressed in the combustion literature [64,66].
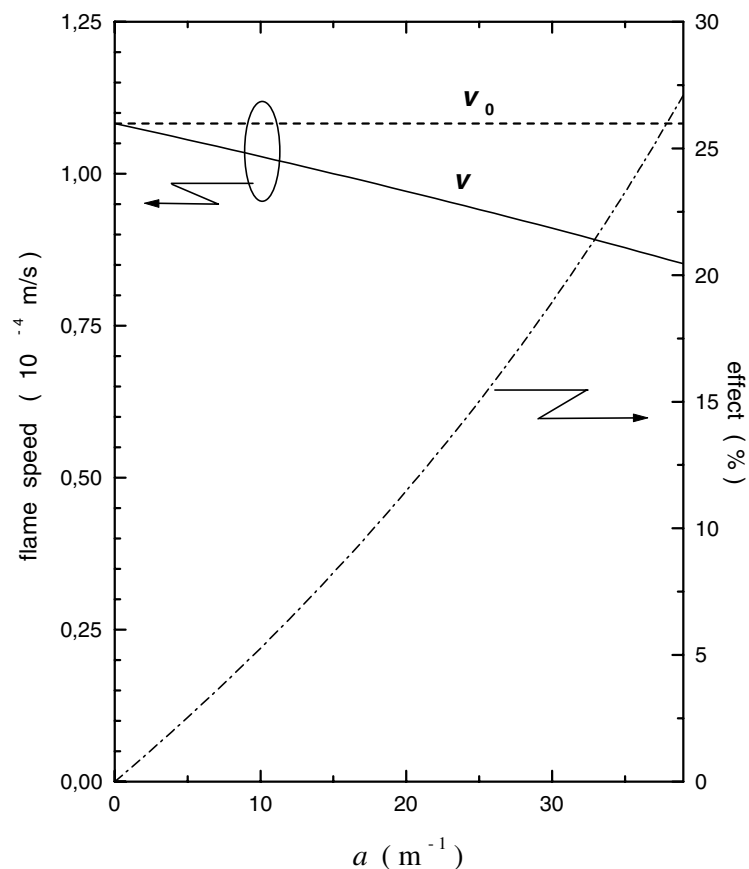
Figure 2. Comparative plot of the predictions for the speed of combustion wavefronts as a function of the absorption coefficient. The dashed curve corresponds to neglecting radiative heat losses, equation (89). When radiative heat losses are included (full curve), the propagation speed is lower because part of the energy from the exothermic reaction is carried away by photons (equation (88)). The dot–dashed curve is the effect of radiative losses, $(v_0 - v)/v$, in %. The values of the parameters are $E_a = 3.1 \times 10^4$ cal mol^{-1}, $\tilde{A} = 7 \times 10^7$ s^{-1}, $Q = 2 \times 10^7$ J kg^{-1}, $T = 553$ K, $\lambda_B = 0.15$ W (K m)$^{-1}$, $\rho_{\text{solid}} = 400$ kg m^{-3} and $\rho_r c_r = 8.97 \times 10^5$ J (kg K)$^{-1}$.

5. Conclusions

In summary, this paper reports the following results.

(i) A CIT description of reactive–conducting systems with several temperatures and a carrier component (section 2.1).

(ii) An extension of this description in order to take into account the finite speed of thermal signals (section 2.2). As a by-product of this model, we have seen that outside LTE, the generalized temperatures θ of EIT are the relevant thermal fields of the system (equation (51)).

In both sections 2.1 and 2.2, we have been guided by a recent thermodynamical theory of heat transport and energy equilibration in radiation–matter systems [35, 36].

(iii) The model in section 2.1 has been applied to the problem of thermal wavefront propagation (section 3.1). The results have been illustrated for combustion fronts, thereby generalizing

Landau's and Zeldovich's results (figure 1). We have predicted a reduction of the thermal speed due to the energy losses (equation (78)).

(iv) In section 4, we have seen that the order of magnitude of the predicted speed is in agreement with available experimental data for combustion fronts over cellulosic fuels. It has also been shown that the effect of radiative losses can easily be about 15% (see figure 2). Our formalism is not restricted to radiation losses but may be applied, e.g., to include the energy loss due to the collisions of reacting molecules with mesoscopic particles.

(v) The model in section 2.2 has been used to generalize the results of (iii) to the case of time-delayed heat conduction (section 3.2). This leads to the prediction of an additional decrease of the wavefront speed (equation (84)). This time-delayed approach can be useful in forest-fire models, where a delay arises because of the ignition time of green trees [27]. We plan to deal with this application in a future work.

Acknowledgment

References

[1] Hurwitz N, Nelkin M S and Habetler G J 1956 *Nucl. Sci. Eng.* **1** 280
    Corngold M 1959 *Ann. Phys., NY* **6** 368
    Williams M M R 1966 *The Slowing Down and Thermalization of Neutrons* (Amsterdam: North-Holland)
[2] Foley W H and Clarke J H 1973 *Phys. Fluids* **16** 375
    Golobic R A and Nerem R M 1973 *Phys. Fluids* **16** 1622
[3] Ichimaru S 1973 *Basic Principles of Plasma Physics* (New York: Benjamin–Cummings)
[4] Kostin M D 1965 *J. Chem. Phys.* **43** 2679
    Shizgal B 1971 *J. Chem. Phys.* **55** 76
    Shizgal B 1987 *Chem. Phys. Lett.* **138** 65
[5] Peixoto J P and Oort A H 1984 *Rev. Mod. Phys.* **56** 365
[6] Mahadevan R 1998 *Nature* **394** 651
    See also Shapiro S L, Lightman A P and Eardley D M 1976 *Astrophys. J.* **204** 187
    Narayan R and Krolik J 1977 *Astrophys. J.* **486** 268
[7] Brorson S D, Fujimoto J G and Ippen E P 1987 *Phys. Rev. Lett.* **59** 1962
    Qiu T Q and Tien C L 1992 *Int. J. Heat Transfer* **35** 719
    Qiu T Q and Tien C L 1993 *J. Heat Transfer* **115** 835
    Qiu T Q and Tien C L 1993 *J. Heat Transfer* **115** 842
[8] Lutgen S *et al* 1996 *Phys. Rev. Lett.* **77** 3657
    Bobylev A V, Potapenko I F and Sakanaka P H 1997 *Phys. Rev.* E **56** 2081
    Ng A, Forsman A and Chiu G 1998 *Phys. Rev. Lett.* **81** 2914
[9] Cukrowski A S, Fritzsche S and Popielawski J 1991 *Far-From-Equilibrium Dynamics of Chemical Systems: Proc. 2nd Int. Symp. (Swidno, 1990)* ed J Popielawski and J Gorecki (Singapore: World Scientific) p 91
    Cukrowski A S, Popielawski J, Qin L and Dahler J S 1992 *J. Chem. Phys.* **97** 9086
    Cukrowski A S, Fritzsche S and Stiller W 1994 *Chem. Phys.* **181** 7
[10] Cukrowski A S 2000 *Physica* A **275** 134
[11] Kumar K 1984 *Phys. Rep.* **112** 319
[12] Vikhrenko V S *et al* 1999 *J. Chem. Phys.* **110** 5273
     Vikhrenko V S *et al* 1999 *J. Chem. Phys.* **110** 5286
[13] Woods L C 1986 *The Thermodynamics of Fluid Systems* (Oxford: Clarendon) chapter 3
[14] DeGroot S R and Mazur P 1984 *Non-Equilibrium Thermodynamics* (New York: Dover)
[15] Jou D, Casas-Vázquez J and Lebon G 1996 *Extended Irreversible Thermodynamics* (Berlin: Springer)
[16] Müller I and Ruggeri T 1998 *Rational Extended Thermodynamics* (Berlin: Springer)
[17] Nettleton R E and Sobolev S L 1995 *J. Non-Equilib. Thermodyn.* **20** 205
     Nettleton R E and Sobolev S L 1995 *J. Non-Equilib. Thermodyn.* **20** 297

Nettleton R E and Sobolev S L 1996 *J. Non-Equilib. Thermodyn.* **21** 1

[18] García-Colín L S, Vasconcellos A R and Luzzi R 1994 *J. Non-Equilib. Thermodyn.* **19** 24

[19] Luzzi R, Vasconcellos A R and Ramos J G 2000 *Statistical Foundations of Irreversible Thermodynamics* (Leipzig: Teubner)

[20] Eu B C 1992 *Kinetic Theory and Irreversible Thermodynamics* (New York: Wiley)

[21] Fort J, Casas-Vázquez J and Méndez V 1999 *J. Phys. Chem.* B **103** 860

[22] Méndez V and Fort J 1999 *Phys. Rev.* E **60** 6168

[23] Cukrowski A S, Popielawski J, Schmidt R and Stiller W 1988 *J. Chem. Phys.* **89** 197
Stiller W, Scmidt R, Popielawski J and Cukrowski A S 1990 *J. Chem. Phys.* **93** 2425 and references therein

[24] Lifshitz E M and Pitaevskii L P 1993 *Physical Kinetics* (Oxford: Pergamon)

[25] Stiller W 1989 *Arrhenius Equation and Non-Equilibrium Kinetics* (Leipzig: Teubner)

[26] Zeldovich Ya B, Barenblatt G I, Librovich V B and Makhviladze G M 1985 *The Mathematical Theory of Combustion and Explosions* (New York: Consultants Bureau)

[27] Méndez V 1998 *Phys. Rev.* E **57** 3622

[28] Sobolev S L 1991 *Sov. Phys.–Usp.* **34** 217
Sobolev S L 1993 *J. Physique* **2261**
Sobolev S L and Manelis G B 1994 *Chem. Phys. Rep.* **13** 878

[29] Murray J D 1993 *Mathematical Biology* (Berlin: Springer)

[30] Gorecki J 1995 *Physica* D **84** 171
Gorecki J and Gorecka J N 1998 *Acta Phys. Polon.* B **29** 455

[31] Lemarchand A and Nowakowski B 1998 *J. Chem. Phys.* **109** 7028
Lemarchand A and Nowakowski B 1999 *J. Chem. Phys.* **111** 6190

[32] Méndez V and Camacho J 1997 *Phys. Rev.* E **55** 6476
Méndez V and Llebot J E 1997 *Phys. Rev.* E **56** 6557
Méndez V and Compte A 1998 *Physica* A **260** 90

[33] Fort J and Méndez V 1999 *Phys. Rev. Lett.* **82** 867
Fort J and Méndez V 1999 *Phys. Rev.* E **60** 5894

[34] Méndez V, Fort J and Farjas J 1999 *Phys. Rev.* E **60** 5231

[35] Fort J and Llebot J E 1996 *J. Phys. A: Math. Gen.* **29** 3427

[36] Fort J, Llebot J E and Pujol T 1999 *J. Phys. A: Math. Gen.* **32** 3095

[37] Sánchez C, Pérez P and Muñoz A 1969 *12th Symp. (Int.) on Combustion (Pittsburgh, PA)* pp 229–40

[38] Prigogine I and Xhrouet E 1949 *Physica* A **15** 913

[39] Sather N F and Dahler J S 1961 *J. Chem. Phys.* **35** 2029
Shizgal B 1980 *J. Chem. Phys.* **72** 3156

[40] Cukrowski A S, Fritzsche S and Haberlandt R 1994 *Ann. Phys., NY* **3** 599
Fritzsche S, Haberlandt R, Michalik H G and Cukrowski A S 1996 *Chem. Phys. Lett.* **259** 331

[41] Costa J, Roura P, Morante J R and Bertran E 1998 *J. Appl. Phys.* **83** 7879

[42] Kennard E H 1938 *Kinetic Theory of Gases* (New York: McGraw-Hill)

[43] Fort J 1997 *Physica* A **269** 439

[44] Truesdell C 1969 *Rational Thermodynamics* (New York: McGraw-Hill)

[45] Landau L D and Lifshitz E M 1959 *Fluid Mechanics* (Oxford: Pergamon)

[46] Nettleton R E 1987 *J. Phys. A: Math. Gen.* **20** 4017
Jou D and Casas-Vázquez J 1992 *Phys. Rev.* A **45** 8371
Hoover W G *et al* 1993 *Phys. Rev.* E **48** 3196
Henjes J 1993 *Phys. Rev.* E **48** 3199
Jou D and Casas-Vázquez J 1993 *Phys. Rev.* E **48** 3196
Casas-Vázquez J and Jou D 1994 *Phys. Rev.* E **49** 1040
Eu B C and García-Colín L S 1996 *Phys. Rev.* E **54** 2501
Luzzi R *et al* 1997 *Physica* A **234** 699
Fort J *et al* 1998 *Physica* A **248** 97

[47] Cukrowski A S, Fritzsche S and Handerlandt R 1994 *Ann. Phys., Lpz.* **3** 599

[48] Cukrowski A S, Fort J and Fritzsche S 1997 *Polish J. Chem.* **71** 1718

[49] Di Bartolo S J and Dorsey A T 1996 *Phys. Rev. Lett.* **77** 4442

[50] Bhattacharjee S and Altenkirch R A 1992 *Proc. 24th Symp. (Int.) on Combustion (Pittsburgh, PA)* pp 1669–76

[51] Williams F A 1985 *Combustion Theory* (Reading: Preseus) equations (E.50), (8.9) and (8.26)

[52] Essex C 1984 *Astrophys. J.* **285** 279

[53] Essex C 1984 *Planet. Space Sci.* **32** 1035

[54] Essex C 1984 *J. Atm. Sci.* **41** 1985

[55] Essex C 1990 *Advances in Thermodynamics* vol 3 (New York: Taylor and Francis) p 435

[56] Pujol T and Llebot J E 1998 *J. Non-Equilib. Thermodyn.* **23** 62

[57] Pujol T and Llebot J E 1999 *Q. J. R. Meteor. Soc.* **125** 79

[58] Planck M 1991 *The Theory of Heat Radiation* (New York: Dover)

[59] For a detailed review, see Browne F L 1958 Theories of the combustion of wood and its control *US Forest Production Laboratory Report* 2136 Madison http://www.fs.fed.us/

[60] Ragland K W and Aerts D J 1991 *Biores. Tech.* **37** 161

[61] Lide D R (ed) 1993 *CRC Handbook of Chemistry and Physics* 74th edn (Boca Raton, FL: Chemical Rubber Company)

[62] Maunuksela J *et al* 1997 *Phys. Rev. Lett.* **79** 1515

[63] Frey and T'ien 1976 *Comb. Flame* **26** 257

[64] Ronney P D 1998 *Proc. 27th Symp. (Int.) on Combustion (Pittsburgh, PA)* pp 2485–506

[65] LeVan 1985 *J. Fire Sci.* **3** 208

[66] Ju Y, Masuya G and Ronney P D 1998 *Proc. 27th Symp. (Int.) on Combustion (Pittsburgh, PA)* pp 2619–26

[67] Sivashinsky G I 1974 *Int. J. Heat Mass Transfer* **17** 1499

[68] Joulin G and Clavin P 1976 *Acta Astronaut.* **3** 223

[69] Mitani T 1980 *Comb. Sci. Tech.* **23** 93